

Deep seismic imaging in the presence of heterogeneous overburden: Insights from numerical modeling

M. Yoon, S. Buske, and S. A. Shapiro

email: yoona@geophysik.fu-berlin.de

keywords: *prestack depth migration, heterogeneous overburden, scattering, amplitude fluctuation*

ABSTRACT

Seismic scattering occurs due to the interaction between elastic waves propagating through the earth and the heterogeneities within. Depending on the scattering strength the reflections from structures below heterogeneous regions suffer from signal distortion and amplitude loss. In order to qualitatively analyze the image distortion in the presence of a heterogeneous overburden migrated sections have been numerically calculated and analyzed. First results show that weak scattering in the overburden slightly increases the image quality of structures below, an increase of the maximum reflectivity was observed for weak fluctuation 1%, independently from the correlation lengths of the heterogeneities. With increasing variances the reflectivity of the deep targets were decreased, until an apparent total loss in the way that strong scattering prevents imaging of deeper structures. Further numerical studies of the relationship between image distortion and the thickness of the random layer, the aspect ratio of the heterogeneities correlation lengths, and the ratio between the correlation length and the wavelengths are necessary to provide a deeper understanding of the scattering influence on deep seismic images.

INTRODUCTION

Seismic scattering occurs due to the interaction between elastic waves propagating through the earth and the heterogeneities within. Depending on the scattering strength the reflections from structures below heterogeneous regions suffer from signal distortion and amplitude loss. Consequently, seismic imaging of these reflection events becomes a difficult task. The reflections can even vanish completely leading to false conclusions, because deeper structures are apparently not observed. This issue plays an important role for structural and geodynamic interpretation of seismic depth sections in complex regions with strongly scattering areas, e.g. the imaging of sub-basalt targets. Thus, understanding scattering phenomena and their impact on the seismic image is of ongoing interest, not only in exploration seismic surveys, but also for deep seismic reflection projects, where the crustal and the upper mantle structures are the main targets.

The prestack migrated depth section of the ANCORP line is one example of a deep seismic reflection line over a strongly heterogeneous environment (Fig. 1) (Yoon et al., 2003). The data set has been acquired to investigate the geodynamic processes in the Central Andes (ANCORP Working Group, 2003). The ANCORP data set provides a detailed image of the subduction zone at 21° S, revealing reflections of crustal structures e.g. the Quebrada Blanca Bright Spot (QBBS) and the Altiplano reflectors, as well as of the subducting Nazca plate at depths between 40 km down to 80 km. The apparent breakdown of the Nazca reflector below the QBBS at a depth of around 80 km and the finding of a reasonable interpretation of its geological nature are still subjects of ongoing studies. A reflectivity analysis of the QBBS and the Nazca reflector showed a very complex reflection pattern for both features. A statistical analysis of the reflection polarity distribution of the Quebrada Blanca Bright Spot did not provide indications for a clear geologic interpretation (ANCORP Working Group, 2003). One reasonable interpretation could be that the QBBS is a large complex system of granitic intrusions or a zone where ascending fluids are trapped and

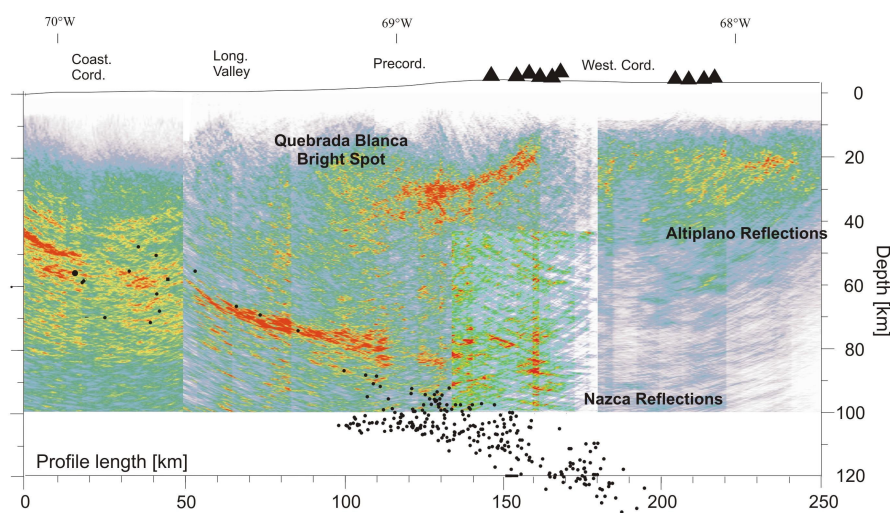


Figure 1: The prestack depth migrated section of the ANCORP96 deep reflection profile reveals a complete image of the subducting Nazca reflector down to depths greater than 80 km. It shows that below strongly scattering structures, e.g. Quebrada Blanca Bright Spot the reflectivity decreases and becomes strikingly weak. It vanishes completely below the Altiplano region in the eastern part of the section.

accumulated. The latter explanation requires low resistivities at the QBBS, but results from magnetotelluric measurements show contradicting high resistivity anomalies in this region. An appropriate explanation for the weak reflectivity of the deep Nazca reflector might be that the amplitudes of transmitted and reflected energy decrease in the presence of strong scattering structures. Another open question is, whether the seismic image of the Nazca reflector becomes complex due to the influence of the complex overburden (QBBS) or whether the reflector itself is complex, and thus its image.

Similar observations, their interpretations and the better handling of this problem has been the focus of the last decades. The improvement of migration techniques, the enhancement of velocity inversion techniques, as well as the extraction and interpretation of structural parameters have been research subjects in exploration seismics and in crustal seismology (Martini et al., 2001; Henstock and Levander, 2000). Early papers on numerical modeling of wave propagation that take scattering into account were presented by Frankel and Clayton (1984, 1986) and Raynaud (1988). A number of studies investigated scattering in the context of seismic imaging, i.e. reflection and refraction seismic surveys (Gibson and Levander, 1988, 1990; Gibson, 1991). A comprehensive overview is given in Levander and Holliger (1992). An extensive study of imaging crustal structures with randomly distributed heterogeneities was presented by Emmerich et al. (1993). An analysis of prestack depth migrated sections revealed that multiple scattering prevents correct imaging of these structures. From the modeling results they recommended a very careful use of commonly applied line drawing techniques, if the imaged region is strongly heterogeneous. They also concluded that the determination of heterogeneities orientations from seismic images is less reliable than commonly assumed. The extraction of statistical parameters i.e. variance and correlation lengths of the heterogeneities have become the subject of later papers. The determination of these parameters provides the basis for possible amplitude and travel time corrections of seismic data prior to imaging procedures (Buske et al., 2001). A number of studies based on borehole data analyses revealed that the variances of velocity fluctuations found in the crust show significant variation with region and with depth (Holliger and Levander, 1994; Frenje and Juhlin, 1998). Typical values for velocity fluctuation in the crust are around 4%. Dolan et al. (1998) proposed that correlation lengths in the upper crust are on the order of kilometers with aspect ratios of about 4. Other studies proposed aspect ratios smaller than 2 for the upper crust (Wu et al., 1994). The accuracy and the reliability of extraction methods and the extracted values is still rather questionable, as they appear to be strongly dependent on the data type and the frequencies contained in the data (Pullammanappallil et al., 1997; Bean et al., 2001). Also, Hurich (1996) found out by studying

the wave field in weak and strong scattering regimes, that wave fields in the strong scattering regime show shorter lateral correlation lengths than expected. He came to the conclusion that the strong scattering component becomes dominant in situations where weak and strong scattering is present, thus biasing the correlation length and the variance extraction analysis.

The present study has been carried out to provide a better understanding of strong scattering present in deep reflection seismic surveys and shows results from numerical modeling. The used synthetic models are related to the ANCORP'96 experiment. A qualitative relationship between the image fluctuation and the heterogeneity in the overburden will be given. The next section gives an introduction to the set-up of the numerical experiments. Section three will present and discuss the modeling results. Finally, a summary and conclusion will be given in section four.

NUMERICAL EXPERIMENTS

In order to qualitatively analyze the image distortion in the presence of a heterogeneous overburden 12 migrated sections have been numerically calculated and analyzed. In the following, the set-up of the numerical experiments will be described e.g. the experimental setting, the finite-difference modeling code, and the prestack depth migration.

Model description

The experimental set-up e.g. receiver and shot point spacing, model size and its structure, as well as the values of the elastic parameters were chosen following the ANCORP'96 profile. The total physical size of the model was $100 \text{ km} \times 90 \text{ km}$ in horizontal and in vertical direction, respectively (see Fig. 2). The

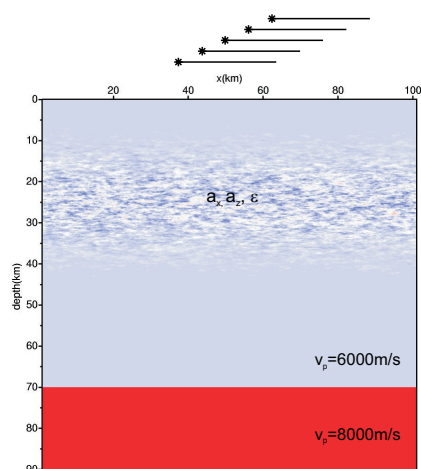


Figure 2: The set of 12 models were build of two homogeneous layers with a 20 km thick random layer which is superposed at depths between 15 km and 35 km . The statistical parameters i.e. the standard deviations and the horizontal correlation lengths of the heterogeneities varied between 1% and 20% and 1000 m and 6000 m , respectively. The vertical correlation length was held constant and was set to 200 m . The layer boundary representing the deep Nazca reflector was at a depth of 70 km . The p wave velocity was 6000 m s^{-1} for the upper layer and 8000 m s^{-1} for the lower one.

velocity model consists of two parts: the 70 km thick upper layer representing the crust and the mantle of the overriding continental plate, that contains an approximately 20 km thick random heterogeneous part. Second, an homogeneous layer that represents the subducting oceanic plate. The random layer was positioned at depths between 15 km and 35 km . For the purpose of image distortion analysis all models were generated with this overall layer geometry, but with varying velocity fluctuations and correlation lengths of the heterogeneities. The vertical and the horizontal correlation lengths were defined independently.

The background P-wave velocity of the upper homogeneous part was set to $v_p = 6000 \text{ m s}^{-1}$, the P-wave velocity of the lower half space was $v_p = 8000 \text{ m s}^{-1}$, respectively. The Poisson's ratio was defined to 0.25. Densities of both layers were derived from the empirical Nafe-Drake relation. The density of the random part was kept constant and was calculated corresponding to the background velocity.

The velocity fluctuations were distributed according to an exponential autocorrelation function. The relative velocity fluctuations were calculated referring to the background velocity of the upper layer. Instead of choosing the von-Karman distribution, which is commonly used to represent the fractal nature of heterogeneous structures in the earth, the limited frequency bandwidth of the data made the choice of an exponential function reasonable. The vertical correlation length was kept constant with $a_z = 200 \text{ m}$, while the horizontal correlation length was set to 1000 m , 4000 m , and 6000 m . The aspect ratios of the horizontal and the vertical correlation lengths in all models were greater than 4 referring to various values from studies of crustal structures (Holliger and Levander, 1992; Dolan et al., 1998). Thus, the heterogeneities are horizontally orientated and therefore resemble horizontal layering. The velocity fluctuations varied between 1%, 5%, 10%, and 20%. The velocity fluctuations were exponentially tapered in the vertical direction.

The parameters used here provided the best compromise between the model size, the computation cost and the modeling constraints e.g. dispersion and stability criterion.

Generation of synthetic depth section

The seismogram sections were calculated using a second-order finite-difference solution of the elastic wave equation based on an implementation by Saenger et al. (2000). The finite difference grid size was 25 m . The dominant frequency of the explosion source wavelet was 12.5 Hz , its maximum frequency 30 Hz . The resulting dominant and minimum wavelengths were about 480 m and 150 m , respectively. The first Fresnel zone W_{Fr} at a depth of 20 km was about ($W_{Fr} \approx 4500 \text{ m}$). For each velocity model 5 shot gathers were calculated as a roll-along profile with a shot point spacing of 6.25 km . The first shot point was set at $x = 37.5 \text{ km}$, the last one at $x = 62.5 \text{ km}$ (Fig.2). 252 Receivers were positioned on the right-hand side of each source location. The receiver spacing was 100 m , which provided a maximum offset of about 25 km . The total recording time of the shot gathers was 30 s . Fig. 3 exemplary shows the main reflection events that were recorded in all seismogram section. The direct wave, the backscattered wave field between 5 s and 15 s two way travel time (TWT) and the deep reflection hyperbola between 23.5 s and 24.5 s TWT. A closer look at the deep reflection event reveals that the coherency of the first arrivals suffer from amplitude and phase fluctuation. A coda with a length of 0.5 s has been generated by the interaction of the propagating wave field with the heterogeneities.

Kirchhoff prestack depth migration

Kirchhoff prestack depth migration was applied to the synthetic data and provided the single shot migrated depth sections (Buske, 1999). No preprocessing such as frequency filtering or muting of the direct wave has been applied to the data prior to migration. The spatial increments were $\Delta x = 100 \text{ m}$ in horizontal direction and $\Delta z = 25 \text{ m}$ in depth, respectively. A constant migration velocity of 6000 m s^{-1} was used. Final stacking of the migrated shot gathers yielded the depth sections for the analysis.

Limitations of the model study

The data processing and the migration have been performed under ideal conditions, i.e. random noise is absent in the data and the velocity distribution is known. Additionally, a model with very simple geometry has been used. Certainly, the model cannot resemble the complex structure of the central Andean subduction zone or other comparable regions with complex geology. Additionally, the receivers were positioned along an ideal line, thus 3D effects from crooked line arrays are also neglected. In real experiments this situation is rarely given, especially in the case of large-distance onshore measurements. Thus, the results from this study cannot provide a complete explanation of the phenomena, which can be observed in real data examples, but they might give qualitative estimations on image distortion and provide constraints for geological interpretations and further investigations.

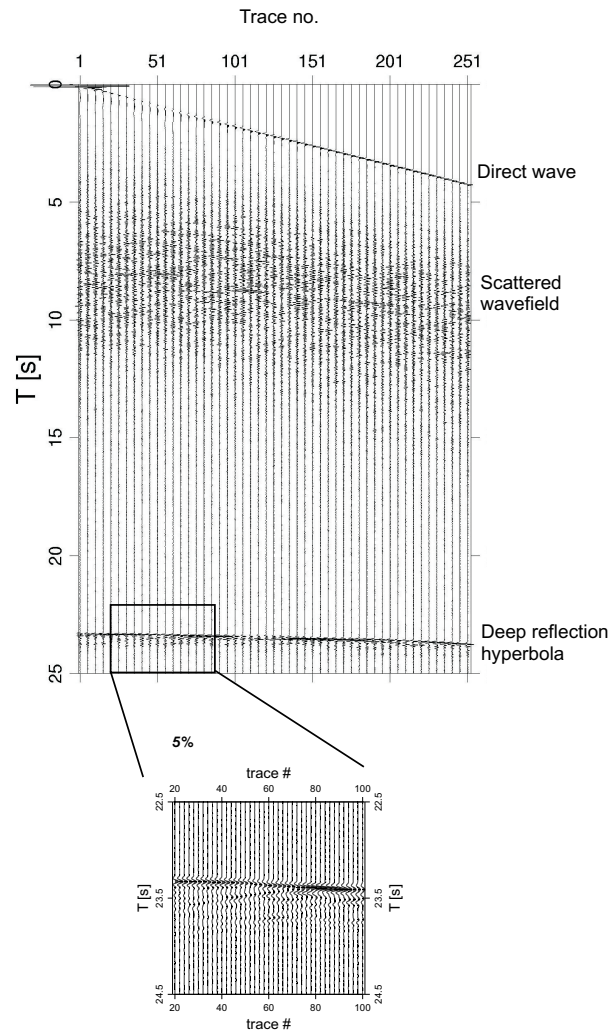


Figure 3: The synthetic seismogram section for the vertical component shows apparently incoherent reflections at TWT 4 s and 12 s. The deeper reflection hyperbola became incoherent due to the heterogeneous overburden. 3b: Zoom - Reflections in the presence of heterogeneities. A closer look at the deeper reflections shows incoherent first arrivals and a coda of 0.5 s duration, generated by multiple scattering in the random layer.

RESULTS

A qualitative and quantitative analysis of the scattering strength in the random layer and the image distortion of the deeper reflector have been performed and will be described in the following. The distortion of reflector images can be described by the change of reflectivity and the degree of reflector image distortion. The 12 final depth sections are shown in Fig. 4. The sections are shown for increasing fluctuation (1%, 5%, 10% and 20%) from left to right and increasing horizontal correlation lengths with 1000 m, 4000 m, and 6000 m, respectively. The vertical correlation length was kept constant with $a_z = 200$ m. The amplitude scaling is equal for all displayed sections.

The images in Fig. 4 present the 30 km wide and 80 km illuminated central parts of the final sections representing the area with the highest subsurface coverage. The focus of the reflectivity analysis was set on these regions. The apparent strong reflections at depths of about 5 km are due to the migration of the direct waves, which have not been muted before migration. The reflectivity of the random layer images at depths between 15 km and 35 km becomes stronger with higher variances. One can observe that the reflections

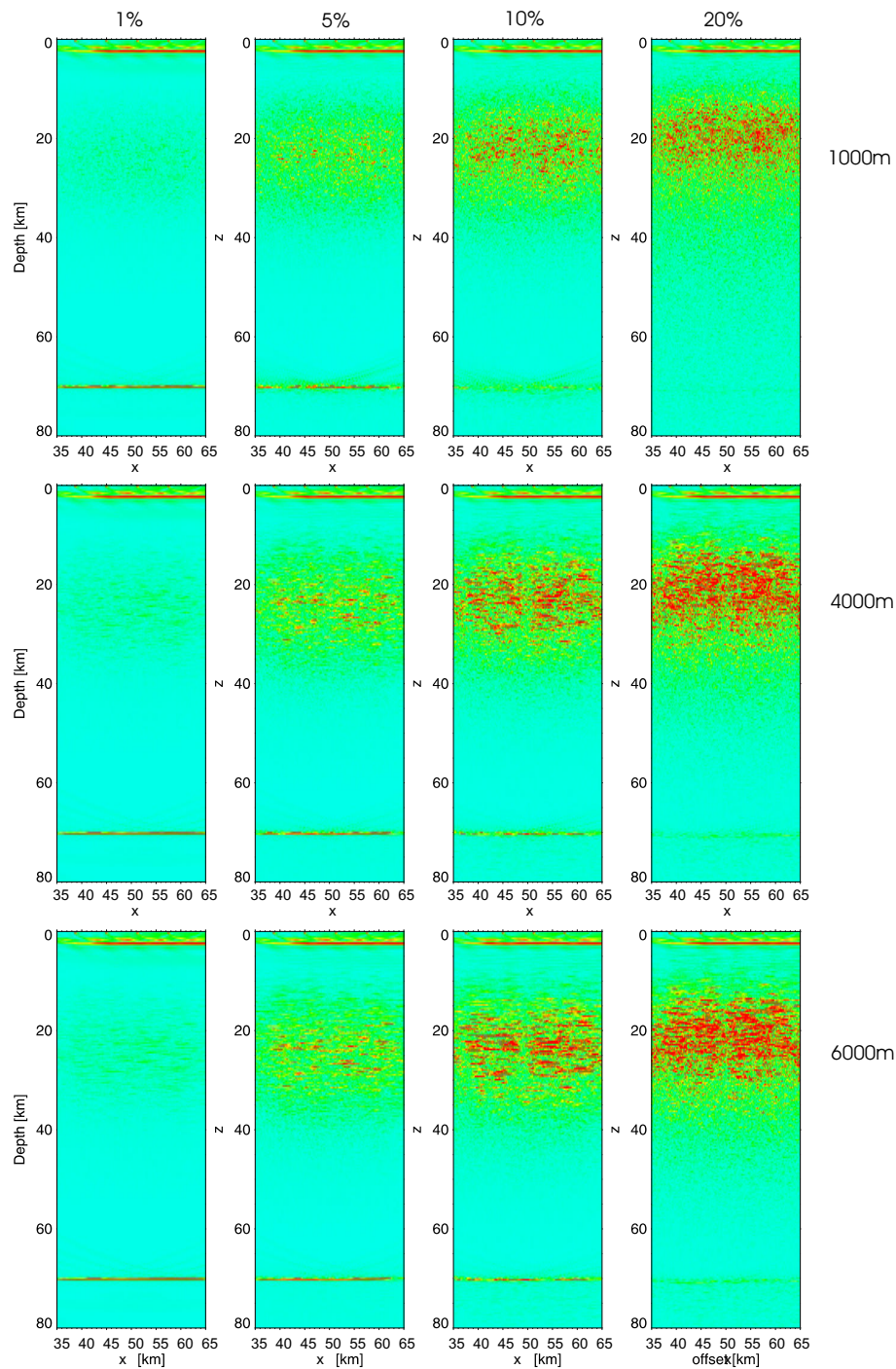


Figure 4: The prestack depth sections are shown for increasing variances from left to right and for increasing horizontal correlation lengths from top to bottom (upper: 1000 m, middle: 4000 m, lower: 6000 m). The reflectivity of the deep reflector decreases with increasing variances and with decreasing horizontal correlation lengths. The reflectivity vanishes almost completely for 20% for all correlation lengths. Also image fluctuation of the reflector geometry increases with shorter horizontal correlation lengths. The influence of the correlation length on the shape of the deep reflector image is small for weak fluctuations (1%) and becomes large for higher variances.

of the random layer resemble the structures of the heterogeneities. The reflection patterns become more and more horizontally aligned towards larger horizontal correlation lengths.

In order to qualify the influence of the random overburden for each depth section the averaged reflection amplitudes of a sub area of the random layer were calculated from the migrated depth sections, as well as the averaged reflection amplitudes along the deep reflector. The average has been calculated after $A_{ave} = \sqrt{\frac{1}{n} \sum_n A_n^2}$.

Fig. 5 shows the averaged reflectivity values at given variances of the central parts of the random

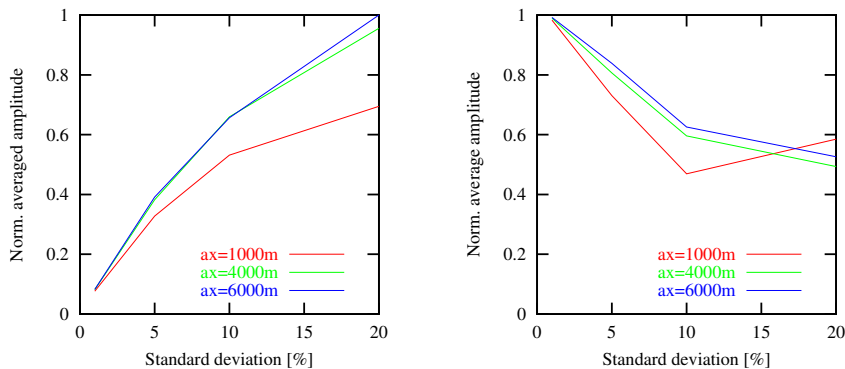


Figure 5: left: Averaged reflectivity in the random overburden. The averaged reflectivity in the random overburden is comparable for weak fluctuations for all horizontal correlation lengths, but becomes stronger for larger lengths with increasing variances. The reflectivity for short correlation lengths is weaker. **right:** Averaged reflectivity of the deep reflectors. The averaged reflectivity along the deep reflector shows a decrease for fluctuations smaller than 10 %.

layer and along the deep reflector. This analysis revealed that in the presence of weak scattering in the overburden, i.e. 1%, the mean reflection amplitudes of the reflector do not change significantly and have the same strength for all correlation lengths. For increasing variances the reflectivity in the random layer increases for all models. Comparison of the depth sections calculated from models with the same variances showed that the reflectivity in the random layer is higher for models with larger horizontal scale lengths. For correlation lengths of $a_x = 4000 m$ and $a_x = 6000 m$, the mean reflectivity in the random layer shows similar amounts of increase. Compared to the latter the increase of reflectivity for the correlation length of about $a_x = 1000 m$ is smaller. The shape of the reflectors shows no significant change in any section for small fluctuations about 1%. For higher variances an increase of image distortion was observed for the deep reflector. A strong decrease of deep reflection strength is observed for fluctuations of about 20%. This might lead to an apparent lack of reflections, if the reflection strength is decreased below the noise level present in real data. Regarding the same standard deviation in the random medium, i.e. 5% and 10%, longer horizontal correlation lengths have smaller effects on the reflection strength of the deep reflector than shorter correlation lengths. In the presence of strong scattering the true geometry of a deep reflector is disturbed. For a correlation length of $a_x = 1000 m$ and 20% velocity fluctuation the reflection strength of the deep reflector has been decreased below a visible level. This leads to the conclusion that in situations where extremely strong scattering is present a strong decrease of reflectivity of structures below the scattering region has to be assumed. Thus, deeper structures cannot be recognized from the reflection image, which possibly might lead to geological misinterpretation.

In order to transfer the results from the numerical modeling on the real data, the synthetic depth sections have been compared to parts of the ANCORP depth section (Fig. 6). The areas of main interest are the regions between 120 km – 160 km and 200 km – 240 km of the profile. These parts contain the strongly scattering QBBS and the Altiplano reflectors at depths between 20 km – 40 km. Both are supposed to effect the structural images beneath. A qualitative comparison of the depth image between 120 km – 160 km with

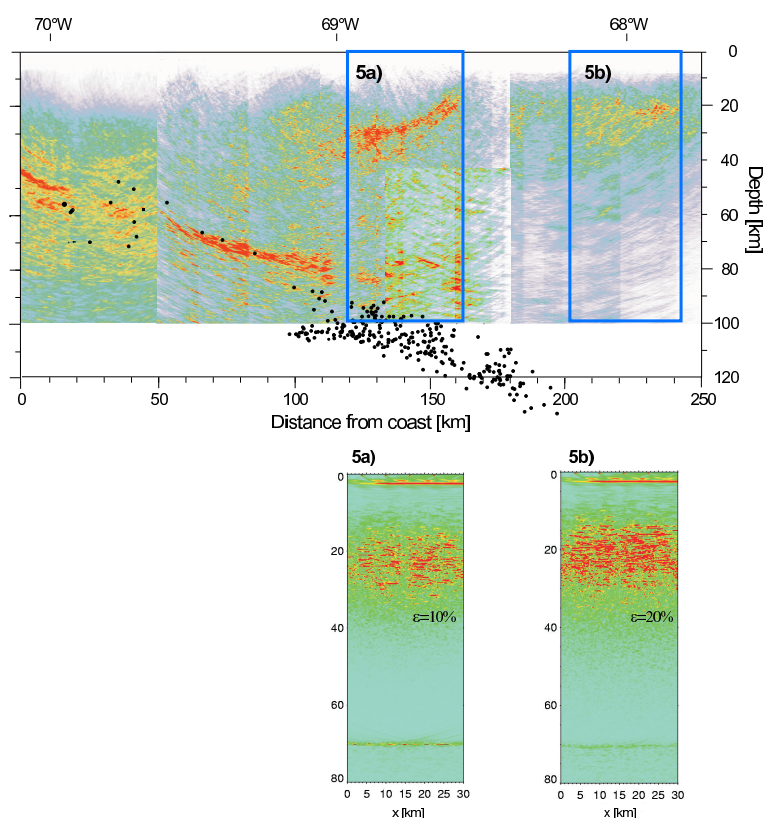


Figure 6: Modeling results suggest that the breakdown of the Nazca reflectivity below the Quebrada Blanca Bright Spot between 110 km and 160 km of the profile is due to strong scattering structures. The standard deviation might be about 10% of the latter, thus that reflectivity of the down going plate is weakened. Comparison of modeling results with the migrated real data shows that a 20 km thick highly scattering (20%) complex zone can lead to a complete loss of reflection energy. Thus possibly existing structures below cannot be imaged.

the synthetic sections indicate that an overburden with 10% velocity variance might weaken the reflectivity of deeper structures in the way as it can be observed in the real dataset (Fig. 6a). Furthermore numerical modeling suggests that the Altiplano reflectors can be considered as region containing heterogeneities of about 20% (Fig. 6b). A high loss of reflection energy might take place due to strong multiple scattering in that region, which might be a possible explanation for the missing deeper structural images below.

An extraction of statistical parameters such as variance and correlation lengths directly from the AN-CORP data was not performed since the data quality was not sufficient. This is mainly due to the low data coverage, a low signal-to-noise ratio of the data, as well as due to 3D effects caused by a strongly crooked profile line.

SUMMARY AND CONCLUSION

The presented numerical modeling results show that the presence of a heterogeneous overburden strongly influences reflection seismic images of deeper structures. In dependence on the correlation lengths and the variances in the random overburden, the migrated images of deeper reflectors are weakened in reflectivity and the shapes are distorted, especially for high velocity fluctuation.

12 depth sections were generated and analyzed regarding the shape and the strength of reflections within. The synthetic seismograms were calculated by an implementation of a finite-difference scheme. A constant velocity Kirchhoff prestack depth migration provided the synthetic depth sections. All models had identical sizes and structures, an upper homogeneous part containing a random layer of 20 km height

and a lower half space. The amplitudes of the variances and the horizontal correlation lengths of the heterogeneities located in the upper random layer were varied, but the vertical correlation length was kept constant. The correlation lengths were in the order of the dominant wavelength of the source wavelet.

Studying the calculated depth sections revealed that the images of the deep reflectors were slightly distorted but the imaged shape of the layer resembled the true geometry of the reflection boundary. This could be observed even for standard deviation larger than 10%, independent from the horizontal correlation lengths. The degree of image distortion is dependent on the variance and on the ratio of the dominant wavelength to the horizontal correlation length of the heterogeneities. Modeling showed that large-scale heterogeneities have a smaller influence on the image distortion of the deep reflector, although scattering in the overburden is stronger.

The results show that weak scattering in the overburden slightly increases the image quality of structures below, an increase of the maximum reflectivity was observed for weak fluctuation 1%, independently from the correlation lengths. With increasing variances the reflectivity of the deep targets were decreased, until an apparent total loss in the way that strong scattering prevents imaging of deeper structures. This should be kept in mind when interpreting crustal data or images of structures buried in complex heterogeneous areas, especially when using AVO analysis for structural interpretation.

The modeling results indicate that the apparent weak reflectivity of the Nazca reflector (ANCORP96) and its diffuse image might be caused by the loss of seismic reflection and transmission energy due to effect of scattering in the upper continental crust, i.e. the highly reflective QBBS. The results also give indications that the high reflectivity of the Altiplano might cause the apparent lack of reflection images from structures below. Both structures seem to have strong screening effects on the seismic transmission, causing amplitude decrease up to total loss of reflections.

Further numerical studies of the relationship between image distortion and the thickness of the random layer, the aspect ratio of the heterogeneities correlation lengths, and the ratio between the correlation length and the wavelengths are necessary to provide a deeper understanding of the scattering influence on deep seismic images. Also, the frequency dependent reflection pattern and reflectivity in the low frequency range are subjects for further modeling studies.

ACKNOWLEDGEMENTS

This work was kindly supported by the sponsors of the *Wave Inversion Technology (WIT) Consortium*, Berlin, Germany.

REFERENCES

- ANCORP Working Group (2003). Seismic imaging of an active continental margin in the central Andes (Andean Continental Research Project 1996 (ANCORP '96)). *J. Geophys. Res.*, 108:2328, 10.1029/2002JB001771.
- Bean, C., Marsan, D., and Martini, F. (2001). Statistical measures of crustal heterogeneity from reflection seismic data: The role of seismic bandwidth. *Geophys. Res. Lett.*, 26:3241–3244.
- Buske, S. (1999). Three-dimensional pre-stack Kirchhoff migration of deep seismic reflection data. *Geophys. J. Int.*, 137:243–260.
- Buske, S., Müller, T., Sick, C., Shapiro, S., and Yoon, M. (2001). True amplitude migration in the presence of a statistically heterogeneous overburden. *Journal of Seismic Exploration*, 10:31–40.
- Dolan, S., Bean, C., and Riollot, B. (1998). The broad-band fractal nature of heterogeneity in the upper crust from petrophysical logs. *Geophys. J. Int.*, 132:489–507.
- Emmerich, H., Zwieliich, J., and Müller, G. (1993). Migration of synthetic seismograms for crustal structures with random heterogeneities. *Geophys. J. Int.*, 113:225–238.
- Frankel, A. and Clayton, R. (1984). A finite difference simulation of wave propagation in two-dimensional random media. *Bull. seism. Soc. Am.*, 74:2167–2186.

- Frankel, A. and Clayton, R. (1986). Finite difference simulations of seismic scattering: Implications for the propagation of short-period seismic waves in the crust and models of crustal heterogeneity. *J. Geophys. Res.*, 91:6465–6489.
- Frenje, L. and Juhlin, C. (1998). Scattering of seismic waves simulated by finite difference modelling in random media: application to the Gravberg-1 well, Sweden. *Tectonophysics*, 293:61–68.
- Gibson, B. (1991). Analysis of lateral coherency in wide-angle seismic images of heterogeneous targets. *J. Geophys. Res.*, 96(B6):10261–10273.
- Gibson, B. and Levander, A. (1988). Modeling and processing of scattered waves in seismic reflection surveys. *Geophysics*, 53(4):466–478.
- Gibson, B. and Levander, A. (1990). Apparent layering in common-midpoint stacked images of two-dimensionally heterogeneous targets. *Geophysics*, 55(11):1466–1477.
- Henstock, T. and Levander, A. (2000). Impact of a complex overburden on analysis of bright reflections: A case study from the Mendocino Triple Junction. *J. Geophys. Res.*, 105(B9):21,711–21,726.
- Holliger, K. and Levander, A. (1992). A stochastic view of lower crustal fabric based on evidence from the Ivera Zone. *Geophys. Res. Lett.*, 19:1153–1156.
- Holliger, K. and Levander, A. (1994). Seismic structure of gneissic/granitic upper crust: geological and petrophysical evidence from the Strona-Ceneri Zone (northern Italy) and implications for crustal seismic exploration. *Geophys. J. Int.*, 119:497–510.
- Hurich, C. (1996). Statistical description of seismic reflection wavefields: a step towards quantitative interpretation of deep reflection profiles. *Geophys. J. Int.*, 125:719–728.
- Levander, A. and Holliger, K. (1992). Small-scale heterogeneity and large-scale velocity structure of the continental crust. *J. Geophys. Res.*, 97(B6):8797–8804.
- Martini, F., Bean, C., Dolan, S., and Marsan, D. (2001). Seismic image quality beneath strongly scattering structures and implications for lower crustal imaging: numerical simulations. *Geophys. J. Int.*, 145:423–435.
- Pullammanappallil, S., Levander, A., and Larkin, S. (1997). Estimation of crustal stochastic parameters from seismic exploration data. *J. Geophys. Res.*, 102:15,269–15,286.
- Raynaud, B. (1988). Statistical modelling of lower-crustal reflections. *Geophys. J.*, 95:111–121.
- Saenger, E., Gold, N., and Shapiro, S. (2000). Modelling the propagation of elastic waves using a modified finite-difference grid. *Wave Motion*, 31(1):77–92.
- Wu, R., Xu, Z., and Li, X. (1994). Heterogeneity spectrum and scale-anisotropy in the upper crust revealed by the German Continental Deep Drilling (KTB) Hole. *Geophys. Res. Lett.*, 21(10):911–914.
- Yoon, M., Buske, S., Schulze, R., Lüth, S., Shapiro, S., Stiller, M., and Wigger, P. (2003). Along-strike variations of crustal reflectivity related to the andean subduction process. *Geophys. Res. Lett.*, 30:10.1029/2002GL015848.